Using CFD to study freeze-lining formation: a collaborative research project between academia and industry

Christian M. G. Rodrigues[1], Menghuai Wu[2*], Mathias Chintinne[3], Anton Ishmurzin[4], Gernot Hackl[4], Clemens Lind[5], Zilong Qiu[6], Muxing Guo[6], Annelies Malfliet[6] and Abdellah Kharicha[2]

[1] Chair of Simulation and Modeling Metallurgical Processes, Metallurgy Department, Montanuniversitaet of Leoben, Leoben, Austria
[2] Christian-Doppler Laboratory for Metallurgical Application of Magnetohydrodynamics, Montanuniversitaet of Leoben, Leoben, Austria
[3] Aurubis-Beerse, Nieuwe Dreef 33, 2340 Beerse, Belgium
[4] Department of Modeling and Simulation, RHI Magnesita, Magnesitstrasse 2, 8700 Leoben, Austria
[5] Marketing & Solutions Non-Ferrous Metallurgy, RHI Magnesita, Kranichberggasse 6, 1120 Vienna, Austria
[6] Department of Materials Engineering, KU Leuven, 3001 Leuven, Belgium

[*]E-mail: menghuai.wu@unileoben.ac.at

Abstract. The formation of freeze lining (FL), a protective layer of solidified slag, holds significant economic value in industrial processes by safeguarding furnace reactors and refractories from corrosive molten slag and providing a thermal barrier that minimizes energy consumption. To deepen our comprehension of FL formation, a collaborative research project has been undertaken, bringing together academic partners from the University of Leoben (Austria) and the University of Leuven (Belgium), alongside industrial partners RHI Magnesita and Aurubis-Beerse. This collaboration has led to the development of a novel computational fluid dynamic (CFD) model capable of simulating FL formation across a broad range of applications. The model has undergone rigorous testing, ranging from controlled laboratory experiments to industrial processes, that validated its robustness and versatility. This model framework provides a solid foundation that should be expanded with new fundamental knowledge of FL formation and validated in other relevant industrial settings.

1. Introduction

In the high-temperature world of pyrometallurgy, furnaces often rely on a special natural protective layer called freeze lining (FL). This layer forms when molten slag solidifies on the furnace wall, creating a built-in barrier that protects the furnace and refractories from thermal damage and chemical attack. This not only extends their lifespan but also helps to conserve energy and maintain efficient throughput. The FL technology has proven successful in a wide range of industrial processes, including copper [1,2], lead [3], and ilmenite smelting [4], zinc fuming [5], aluminum production (Hall-Heroult process) [6], and even in steelmaking [7].

Despite its industrial importance, the exact mechanism governing FL formation is not fully understood. Researchers have turned to low-temperature model cells under natural [1] and forced convection [8] to investigate FL behaviour through in-situ observations. They identified bath temperature, composition, and transient mass transfer as critical factors influencing FL thickness. Interestingly, while the main solidified core remained virtually motionless, detached crystals were observed when natural convection conditions were assumed.

Beyond the low-temperature model cells, laboratory experiments have provided valuable insights into the microstructure of FLs. The microstructure analysis of as-solidified samples revealed two distinct zones: a stagnant FL zone and a mobile crystal zone [9]. In the mobile zone, crystals were transported towards or away from the FL (depending on the flow direction), while solidifying and growing. Interestingly, factors like agitation [10], lower slag viscosity [11], and different slag systems [12] all eliminated the mobile zone. A separate rheological study [13] demonstrated a sharp increase in viscosity with increasing solid fraction, suggesting a transition from a liquid-like to a solid-like state. This transition marked the location of the FL front, where the temperature remained below the liquidus temperature [11, 13]. Similar to cold experiments, FL thickness was not solely governed by thermodynamic equilibrium. Instead, it depended on a complex interplay of crystallization, transport, and remelting mechanisms occurring within a liquid boundary layer ahead of the FL [11].

Despite ongoing research, modelling FL formation remains in its infancy. Numerical models can offer valuable insights into specific mechanisms occurring during FL formation. However, a unified model was still lacking in the literature. To bridge this gap, a collaborative research project has been undertaken to develop a novel CFD model framework capable of simulating FL formation across various applications based on the prevalent literature knowledge. This project brings together academic partners from the University of Leoben (Austria) and the University of Leuven (Belgium), alongside industrial partners RHI Magnesita and Aurubis-Beerse. The model was validated against laboratory experiment (finger experiment) and industrial processes (electric smelting furnace and slag fuming furnace).

2. Model description

The model framework used in all test cases employed a mixture continuum (MC) model to simulate slag solidification (i.e., FL formation). This approach describes the solid/liquid distribution by their respective volume fractions (f_s and f_ℓ), where $f_\ell + f_s = 1.0$. The slag solidification path dictates the temperature-dependent solid fraction. The evolution of the solid fraction directly affects parameters like latent heat transfer during solidification/remelting, drag forces, and material properties (e.g., viscosity). Within the liquidus-solidus temperature range, the solidifying slag forms a mushy zone that is treated as a porous medium. Currently, the as-solidified structure is assumed as a stationary, interconnected network (i.e., no mobile phase is considered).

To ensure accurate modelling of FL formation across different scenarios, the coupling between the MC model and the CFD model was adapted. Details of these adaptations are provided in the corresponding papers [14, 15]. Here, only a brief overview is given.

2.1 Coupling with single-phase model

For scenarios where molten slag directly solidifies into a FL, the MC model was coupled with a single-phase CFD model. This approach was used to simulate FL formation in two distinct cases: the finger experiment conducted in KU Leuven and the electric smelting furnace [14]. Data for

the finger experiment, including boundary conditions and domain dimensions, was directly obtained from the laboratory experiments. Data for the electric smelting furnace simulation was compiled from relevant literature sources.

2.1 Coupling with multiphase VOF model

For scenarios where slag and another fluid interact before FL formation, the MC model was coupled with a multiphase Volume-of-Fluid (VOF) model. This approach was used to simulate FL formation during the slag fuming process [15]. Here, intense gas-slag interactions occur within the reactor, before slag forms a FL. The VOF model treated the slag and gas phases as immiscible hydrodynamic fluids, characterized by their respective volume fractions (α_{slag} and α_{gas}) where $\alpha_{slag} + \alpha_{gas} = 1.0$. This enabled tracking of the slag/gas interface, which was crucial for capturing splashing events during the slag fuming process.

Capturing FL formation during the slag fuming process required distinct approaches for the slag bath and the freeboard (the region above the bath). In the freeboard, FL forms due to the solidification of splashed liquid droplets colliding with the reactor wall. This creates a zone with coexisting gas and solidifying slag ($\alpha_{slag} < 1.0$), known as slurry zone (i.e. includes gas, liquid slag and solid slag). To accurately capture FL formation in both regions, the model was improved as detailed in [15]. Aurubis-Beerse provided real industrial data of the fumer for the model setup and validation.

3. Results

3.1 Test case 1: Finger experiment

To analyse FL formation under controlled conditions, laboratory experiments, also known as the finger experiments, were conducted at KU Leuven (Figure 1a). This experiment involved introducing a gas-cooled probe into a slag bath, inducing FL formation that grew outward from the probe's surface over time. The crucible housing the slag could be set to static (natural convection) or rotating (forced convection) conditions. During the experiment, the slag bath temperature before and during probe immersion, and the heat fluxes were monitored. The experiments were performed for different immersion times to evaluate the evolution of the FL size over time.

Figure 1 b) compares the evolution of the measured FL size with simulation results and demonstrates a good quantitative agreement. The insets i) to iii) illustrate the solid fraction distribution at three different moments during the immersion of the probe into the slag and depicts the shape evolution of the FL over time. This validation confirms the model's accuracy in a controlled environment.

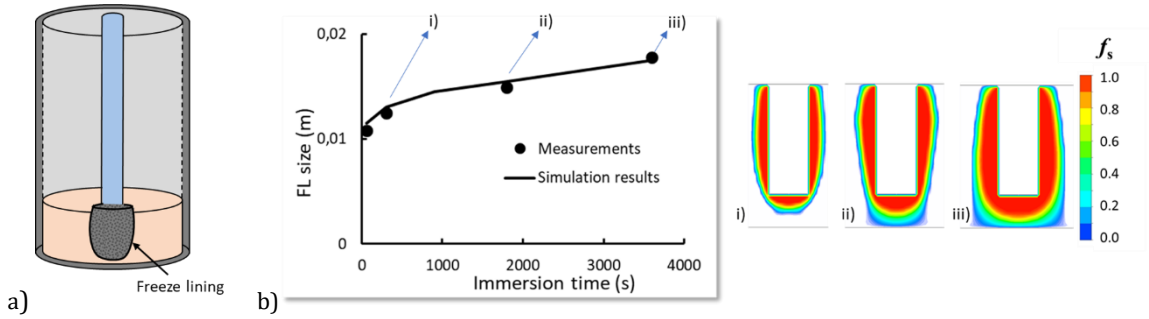

Figure 1. a) Schematic of finger experiment, b) comparison between experimental results and simulation results of FL size over immersion time. The insets in b) show the slag solid fraction distribution, indicating the shape of the FL over time.

3.2 Test case 2: Electric smelting furnace

This case represents an industrial electric smelting furnace for the smelting of nickel matte. The furnace is equipped with six electrodes. A schematic of the cross-sectional view of the furnace (through one of the electrodes) is shown in Fig. 2. During operation, the electrical energy for smelting the feed is generated by Joule heating as the electric current passes between the carbon electrodes and the molten slag bath. After the furnace is charged with the feed, the process produces both slag and a denser nickel-rich layer called matte, which settles at the bottom due to its higher density. The furnace walls incorporate a cooling system (e.g., water-cooled panels) that promotes the FL formation on the interior surface of the furnace/refractory.

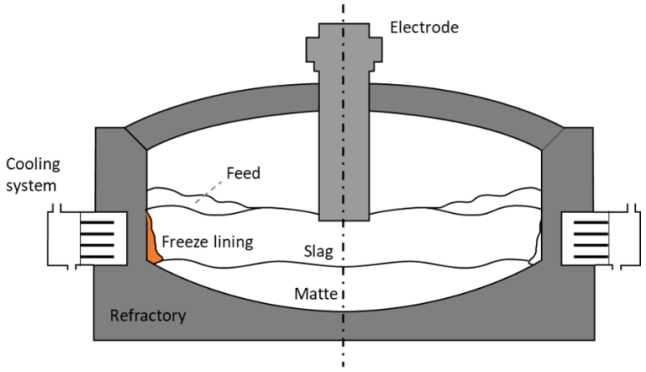

Figure 2. Cross-sectional view of the electric smelting furnace for smelting of nickel matte. The freeze lining location is highlighted.

A crucial aspect of the modelling of the electric smelting furnace involves establishing a valid global energy balance within the furnace. This balance must consider all relevant heat transfer mechanisms occurring during the smelting process, including the effect of FL formation. To capture these mechanisms, several energy source terms were incorporated. These terms account for the input power from the electrodes, heat generated by matte production, heat dissipated due to the presence of the feed during furnace operation, and latent heat released during FL formation.

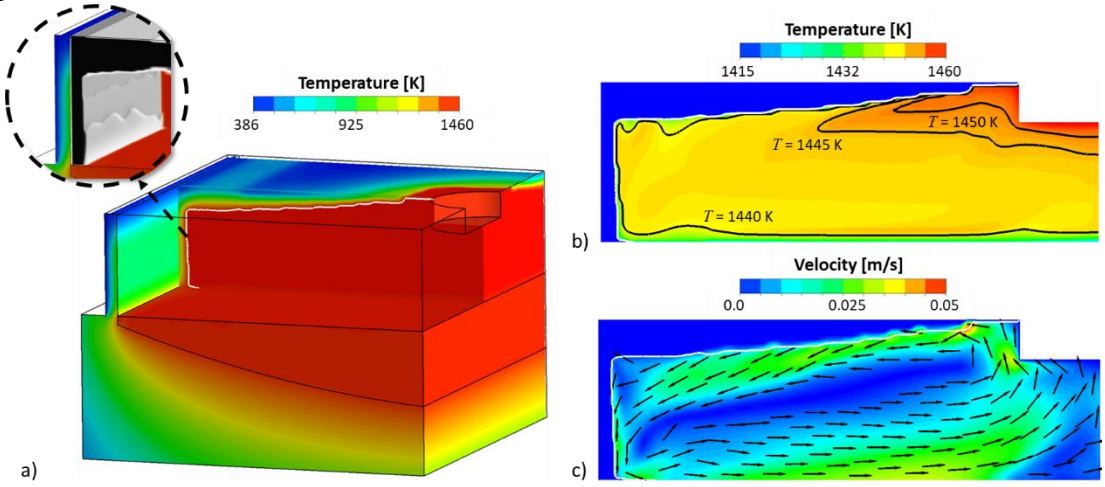

Figure 3. a) Temperature distribution in section of domain, b) temperature distribution with isotherms in 2D plane intersecting electrode, and c) velocity distribution with velocity vectors in 2D plane intersecting electrode. Inset in a) shows dark rendering of FL layer on the water-cooled wall of furnace predicted by the model after reaching a steady-state. Figures taken from [14].

Figure 3 presents the simulation results obtained after reaching a steady-state condition. This means that a thermal balance has been achieved in the system. Figures 3 a) to c) show the temperature distribution in a section of the furnace, the temperature distribution in a 2D plane intersecting an electrode, and the velocity distribution in a similar 2D plane. The inset in Fig. 3 a) highlights the FL layer formed on the water-cooled wall of the furnace.

The vertical black structure illustrated in the inset of Fig. 3 a) confirms the presence of a FL layer on the water-cooled furnace wall. More than a validation of the model for FL formation, these results confirm the successful incorporation of relevant physical phenomena into the model setup. This includes heat transfer from power of the electrodes, heat generated during matte production, heat dissipated due to the presence of the feed and furnace's cooling system, and the latent heat released during FL formation.

The simulations revealed a critical dependence of the FL layer on heat transfer terms. Notably, variations in feed size was clearly associated with different FL thicknesses. Therefore, an accurate estimation of the thermal effect of the feed is critical and must be considered in the global energy balance calculations of the furnace. No data was found in the literature to validate the simulation results.

3.3 Test case 3: Fuming furnace

Aurubis-Beerse operates a zinc recovery process called slag fuming. This innovative technique recycles zinc from slag by relying on submerged plasma torches for a carbon-free energy source. Three of these torches transform compressed air into high-temperature plasma. This plasma is then injected into the molten slag bath, along with a mixture of natural gas and pulverized coal. This gaseous mixture acts as a heat source, stirring force, and reducing agent for ZnO in the fuming process. The resulting zinc fumes are then captured in a baghouse after exiting the furnace. To protect the furnace and its lining (refractories) from the corrosive molten slag, water-cooled jackets are employed around the furnace to promote FL formation. Crucially, industrial data provided by Aurubis-Beerse played a key role in setting up and validating the model. Since the furnace design is 3-fold rotational symmetrical, only one-third of it needs to be considered in the model (as shown in Fig. 4).

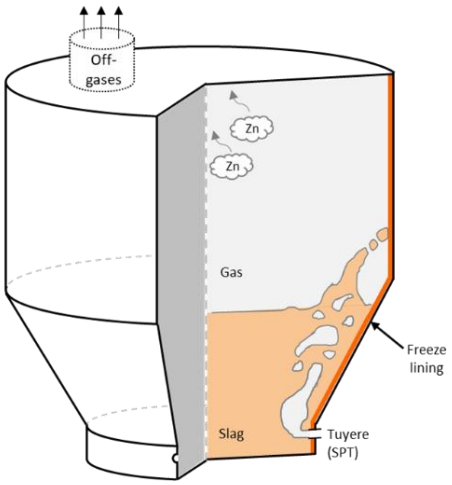

Figure 4. Schematic of the batch-type, plasma-driven slag fuming furnace. Figure taken from [15].

The flow dynamics observed during the slag fuming process are shown in Fig. 5 a). The blue iso-surface, representing the slag/gas interface at $\alpha_{slag} = 0.1$, illustrates the splashing motion of the molten slag across the freeboard. The splashing events are caused by the interaction

between the hot gas plumes (created upon injection through the submerged plasma torches) and the molten slag bath. Figure 5 b) captures a moment just after a previously splashed molten slag layer has solidified in the upper right side of the freeboard. This is confirmed by the f_s colour contour in cyan (which means that it is partially solidified at this moment). This solidification is driven by the heat transfer from the existing, cooler FL layer on the freeboard wall. In contrast, the upper left side of the freeboard shows a fresh splashing event where the slag remains molten (dark blue iso-surface). This highlights the ongoing dynamic interplay between splashing and solidification of the FL layer.

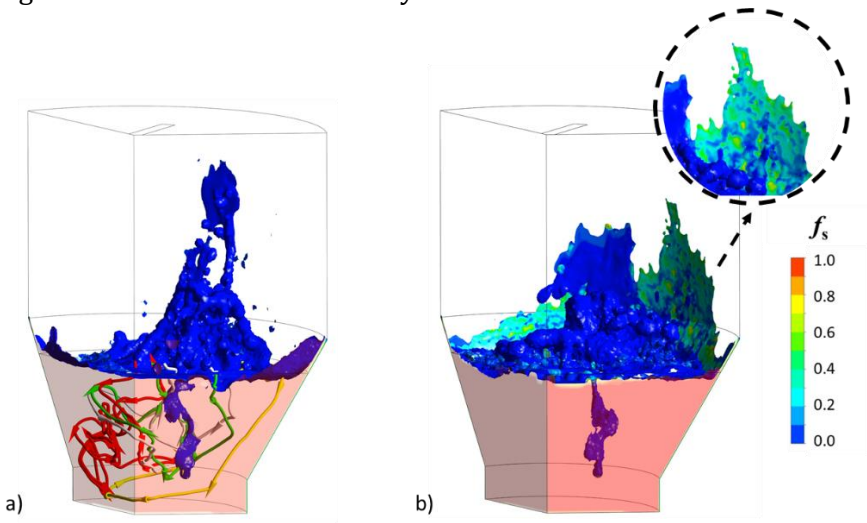

Figure 5. a) Slag splashing and flow in slag bath at t = 180.1 s. The blue iso-surface depicts the slag/gas interface (α_{slag} = 0.1). The semi-transparent red region is the slag bath. The coloured streamlines, originating from four points in the bath, illustrate the flow patterns. b) Splashing and FL formation in freeboard illustrated with iso-surface of f_s at t = 173.9 s. The inset provides a magnified view of the impact region where splashed slag gradually solidifies. Figures taken from [15].

Figure 6 a) and b) show the simulation results of the FL distribution on the reactor wall, and variation of the FL thickness along the reactor height for three angles (φ): 0°, 22°, and 45°.

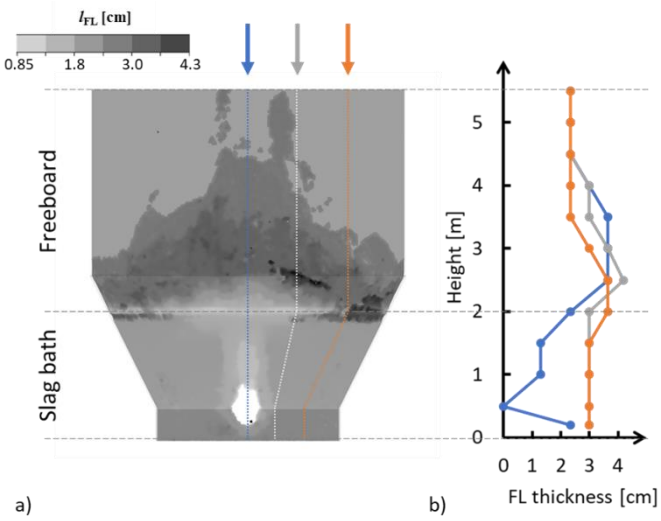

Figure 6. a) FL distribution across the reactor wall, b) FL thickness variation along the reactor height for three azimuthal angles (φ): 45°, 22°, 0°. The 0° azimuthal angle corresponds to the vertical plane

intersecting the centre of the submerged plasma torches. The average measured FL thickness in the industrial furnace operated by Aurubis-Beerse was 3 cm. Figures taken from [15].

In the industrial furnace operated by Aurubis-Beerse, the average measured FL thickness was 3 cm. In the slag bath region (height range between 0 and 2 m in Fig. 6 b)), the simulation results show good agreement with industrial data in regions farther from the submerged plasma torches ($\varphi = 22°$ and 45°). When $\varphi = 0°$, the FL thickness is underestimated because of the simplification made in modelling the submerged plasma torches inlet (to reduce computational cost).

In the freeboard region (height range between 2 and 5.5 m in Fig. 6 b)), the simulation results align reasonably with the industrial data in the regions where enough splashing events have occurred. In regions with not enough splashing, FL is underestimated. More simulation time would be necessary to fully coat the freeboard region.

4. Conclusion

Predicting freeze-lining formation remains a significant challenge due to the complex interplay of physical and chemical processes. FL is critical for designing furnaces and optimizing refractory performance in many industrial processes. Modelling approaches offer a powerful tool to unravel the complex mechanisms governing freeze-lining formation. This paper explores the results of a collaborative effort between academia and industry, aiming to develop a comprehensive model that accurately simulates freeze-lining formation.

The model's capabilities were tested against various scenarios, ranging from simple laboratory experiments with controlled conditions to more intricate and dynamic industrial processes. The positive agreement between simulation results and experimental/industrial data validates the model's accuracy and confirms the success of the collaboration. This success underscores the critical role of collaborative research projects. Academia's more theoretical expertise effectively combined with industry's real-world knowledge, which proved instrumental in gathering the necessary information for model development.

However, the current model framework requires further development to incorporate new fundamental knowledge of FL formation (i.e., FL growth/remelting kinetics, FL formation response to thermal and compositional fluctuations, etc.), integrate a more complex microstructure (i.e., mobile phase ahead of the FL front observed in some experiments), and validate its effectiveness in other relevant industrial applications. By promoting further collaboration and leveraging the strengths of all the parties involved, a comprehensive model can be developed to achieve a deeper understanding of freeze-lining formation, potentially leading to optimized furnace and refractory designs and improved efficiency in industrial processes.

Acknowledgments

This study was supported by the Austrian Research Promotion Agency (FFG) under the framework of Bridge 1 program (MoSSoFreez Project, F0999888120). We acknowledge Dr. Samant Nagraj, formerly from Aurubis-Beerse, for his valuable input.

References

[1] Guevara F and Irons G 2011 *Metall. Mater. Trans. B* **42** 652-663, doi: 10.1007/s11663-011-9524-3

[2] Campforts M, Verscheure K, Boydens E, Van Rompaey T, Blanpain B and Wollants P 2008 *Metall. Mater. Trans. B* **39** 408-417, doi: 10.1007/s11663-008-9141-y
[3] Swinbourne D 2010 *Miner. Process Extr. Metall.* **119(3)** 182, doi: 10.1179/037195510X12804985731362
[4] Zietsman J and Pistorius P 2006 *Minerals Engineering* **19** 262-279, doi: 10.1016/j.mineng.2005.06.016
[5] Verscheure K, Van Camp M, Blanpain B, Wollants P, Hayes P and Jak E 2007 *Metall. Trans. B*, **38** 21-33, doi: 10.1007/s11663-006-9010-5
[6] Wong C, Bao J, Skyllas-Kazacos M, Welch B, Mahmoud M, Arkhipov A andAhli N 2023 *Metall. Mater. Trans. B* **54** 562, doi: 10.1007/s11663-022-02709-w
[7] Mills K, Su Y, Fox A, Li Z, Thackray R and Tsai H 2005 *ISIJ Int.* **45** 619-633, doi: 10.2355/isijinternational.45.619
[8] Crivits T, Hayes P C and Jak E 2018 *Transactions of the Institutions of Mining and Metallurgy* **127(4)** 195-209, doi: 10.1080/03719553.2017.1375767
[9] Fallah-Mehrjardi A, Hayes P C and Jak E 2014 *JOM* **66** 1654-1663, doi: 10.1007/s11837-014-1127-4
[10] Fallah-Mehrjardi A, Hayes P C and Jak E 2013 *Metall. Mater. Trans. B* **44** 1337-1351, doi: 10.1007/s11663-013-9925-6
[11] Fallah-Mehrjardi A, Hayes P C and Jak E 2014 *Metall. Mater. Trans. B* **45** 2040-2049, doi: 10.1007/s11663-014-0149-1
[12] Campforts M, Jak E, Blanpain B, Wollants P, 2009 *Metall. Mater. Trans. B*, **40** 619- 631, doi: 10.1007/s11663-009-9256-9
[13] Nagraj S, Chintinne M, Guo M and Blanpain B 2022 *JOM* **74** 274-282, doi: 10.1007/s11837-021-05020-2.
[14] Rodrigues C M G, Menghuai W, Ishmurzin A, Hackl G, Voller N, Ludwig A and Kharicha A, 2023, *Metall. Mater. Trans. B*, **54**, 880–894, doi: 10.1007/s11663-023-02733-4.
[15] Rodrigues C M G, Menghuai W, Chintinne M, Ishmurzin A, Hackl G, Lind C, and Kharicha A (in preparation).